

Diabetes mellitus exacerbates post-myocardial infarction heart failure by reducing sarcolipin promoter methylation

Zhongwei Liu¹, Yong Zhang¹, Chuan Qiu², Haitao Zhu³, Shuo Pan¹, Hao Jia⁴, Hongyan Kang⁵, Gongchang Guan¹, Rutai Hui⁶, Ling Zhu^{1*} and Junkui Wang^{1*}

¹Department of Cardiology, Shaanxi Provincial People's Hospital, Xi'an, Shaanxi Province 710068, China; ²Center for Bioinformatics and Genomics, Department of Global Biostatistics and Data Science, School of Public Health and Tropical Medicine, Tulane University, New Orleans, LA, USA; ³Department of Pediatrics, Northwest Women's and Children's Hospital, Xi'an, China; ⁴International Medical Services, Affiliated Hospital of Northwest University, Xi'an, China; ⁵Department of Cardiology, Heyang County People's Hospital, Weinan, China; ⁶Department of Cardiology, Fuwai Hospital, National Center of Cardiovascular Diseases, Beijing, China

Abstract

Aims Sarcolipin (SLN) is a key regulator of sarcoplasmic reticulum calcium-ATPase (SERCA)2a, which handles intracellular calcium re-uptake. This study was aimed to investigate the involvement of SLN in post-myocardial infarction (MI) heart failure (HF) in diabetes.

Methods and results Diabetes/MI rat models were established. Altered SLN expression in diabetic hearts was screened out by microarray. A myocardiotropic viral vector was used to deliver siRNA to silence SLN. DNA methylation was evaluated by bisulfite sequencing. Cardiac functions were evaluated by invasive haemodynamic examinations. The SERCA2a activity, cytoplasmic calcium concentration ($[Ca^{2+}]_i$), calcium spark, and myocyte contraction were detected. Correlation between HF and diabetes was analysed in a cohort consisted of 101 ST-segment elevated myocardial infarction (STEMI) patients between 2017 and 2019 [53.54 ± 4.64 years old; 61.4% male gender; HbA1c% 6.15 ± 2.00; and left ventricular ejection fraction (LVEF%) 40.64 ± 3.20%]. SLN expression was evaluated in left ventricular tissue sample from six STEMI patients complicated with diabetes and six STEMI patients without diabetes. Expressions of DNA methyltransferase 1a and DNA methyltransferase 3 were reduced in diabetic hearts, leading to down-regulation of SLN promoter methylation, resulting in increased SLN expression in rats. Impaired heart systolic functions were found in experimental diabetic MI rats, which were attenuated by SLN silencing. SERCA2a activity reduction and $[Ca^{2+}]_i$ elevation were attenuated by SLN silencing in diabetic animal hearts and high-glucose incubated primary myocytes. SLN silencing suppressed calcium sparks and improved contraction and sarcoplasmic reticulum calcium re-uptake in high-glucose incubated primary myocytes. Expression of SLN was up-regulated in LV sampled from STEMI patients complicated with diabetes compared with non-diabetic ones ($P < 0.05$). LVEF% was reduced in STEMI patients complicated with diabetes compared with non-diabetic ones ($P < 0.01$). HbA1c% and LVEF% was related ($r = -0.218$, $P = 0.028$). Increased HbA1c% was correlated with reduced LVEF% after adjustment for age, sex, body mass index, cigarette smoking, creatinine, UA, low density lipoprotein, K^+ , Na^+ , and troponin I (adjusted odds ratio = 0.75, 95% confidence interval 0.62–0.90, $P = 0.002$).

Conclusions Diabetes increases the vulnerability of STEMI patients to post-MI HF by down-regulating SLN promoter methylation, which further regulates SERCA2a activity via increasing cardiac SLN expression.

Keywords Diabetes mellitus; Myocardial infarction; Heart failure; Sarcolipin

Received: 26 December 2019; Revised: 29 April 2020; Accepted: 7 May 2020

*Correspondence to: Ling Zhu and Junkui Wang, Department of Cardiology, Shaanxi Provincial People's Hospital, Shaanxi Province, 710068, China. Email: lingzhu2360@163.com; junkuiwang@yeah.net

Introduction

HF is a common complication in patients with acute myocardial infarction (AMI) and considered as one of the most powerful independent predictors of major adverse cardiovascular events.¹ The incidence of diabetes mellitus (DM) has been increasing rapidly due to the spread of high-energy diets and static lifestyles, hazarding the public health worldwide. DM patients suffering an AMI were indicated to show worse outcomes compared with non-diabetic patients.² Particularly, post-MI HF contributed to the elevated mortality rate in AMI patients complicated with DM.³ In our previous investigations, impaired cardiac systolic functions were found in diabetic animals.⁴ Thus, the role of DM in exacerbating left ventricular (LV) dysfunction in post-MI HF is suggested. However, the underlying mechanisms are still not elucidated.

Calcium homeostasis is important for maintaining the normal contraction activities of myocardial fibres. It was suggested disorder of calcium handling was a critical mechanism of HF due to its role in excitation–contraction coupling of cardiac muscle cells.⁵ Sarcoplasmic reticulum (SR) calcium metabolism takes responsibilities in pathophysiology of HF. Acting as the ‘calcium pool’, except for releasing calcium, SR also recycles calcium from cytoplasm through SR calcium-ATPase (SERCA)2a. As a major mediator of cardiac excitation–contraction coupling, impaired SR calcium re-uptake results in depletion of SR calcium, which further leads to cardiac contractility impairments.⁶ Increased inhibition of SERCA2a channel activity and decreased SERCA2a expression were described in failing hearts.⁷

The activity of SERCA2a is modulated by its regulators, namely, phospholamban (PLN, a 52 amino acid residues protein) and sarcolipin (SLN, a 31 amino acid residues protein), via direct physical interactions. SLN was reported to reduce SERCA activity by inhibiting calcium affinity and uncoupling the calcium transportation from ATP hydrolysis.⁸ In addition, SLN was reported to induce superinhibitory effects of PLN on SERCA2a by maintaining the monomer form of PLN.⁹ Notably, dramatic LV contractility loss was reported in generated transgenic animal in which ventricle SLN was over expressed.¹⁰

Our previous investigation observed significant cytoplasmic calcium increasing in ventricle tissue from DM animal model.¹¹ It is known that DM induces specific genome-wide cytosine demethylations. The by-products of uncontrolled hyperglycaemia such as methylglyoxal participate in epigenetic modification by removing methyl residues from 5mc of CpG, regulating gene transcriptions by changing chromatin conformation.¹² In our pilot experiment of whole genome-wide mRNA expression microarray analysis, increased expression of SLN was screened out in DM animal model (*Figure 1*). Thus, it was reasonable for us to speculate that DM might take part in calcium handling disorder-related

cardiac dysfunctions via regulating SLN expression through affecting its promoter methylation.

In the current study, *in vivo*, *in vitro* experiments and cross-sectional cohort study were carried out to investigate whether DM exacerbated post-MI HF. Molecular mechanisms concerning hyperglycaemia-induced alteration of SLN promoter demethylation and SLN-mediated calcium handling dysregulations were also investigated.

Material and methods

Animal experiments

All animal experimental procedures were carried out according to Recommended Guideline for the Care and Use of Laboratory Animals issued by Chinese Council on Animal Research. The protocols regarding animal experiments were approved by the Medical Animal Research Ethics Committee at Xi'an Jiaotong University (Ref. 201806230-R1).

Diabetes model establishment

Sprague–Dawley (SD) rats (male/female = 1:1, 9 weeks old, body weight 250 ± 10 g) were provided by Animal Experimental Center of Xi'an Jiaotong University. Animals were raised in independent polypropylene cages in controlled environment providing a 12-h artificial light/dark cycle, (25 ± 1)°C temperature and (50% \pm 5%) humidity. Animals were free to standard chow and sterile water. Diabetes was introduced by single intraperitoneal injection of STZ (65-mg/kg bodyweight, dissolved in citrate buffer; Sigma-Aldrich) in accordance with our previous investigation.¹³ Blood from tail vein was sampled for blood glucose tests. Fasting blood glucose concentrations were determined by automatic analyser (One Touch SureStep Meter, LifeScan). Glycated haemoglobin (HbA1c%) levels were analysed by EBIO plus glucose analyser (Eppendorf AG).

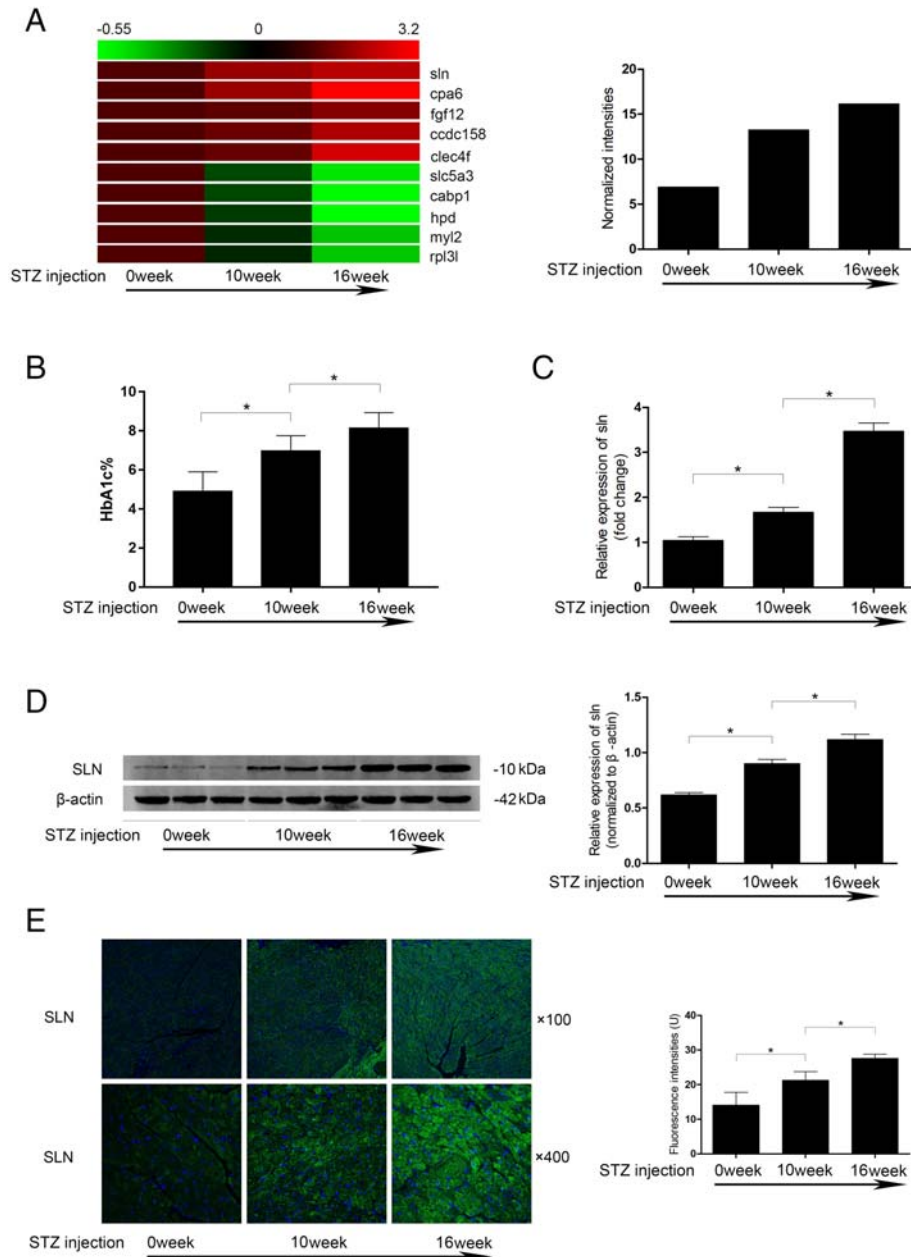
Myocardial infarction model establishment

Rats were anaesthetized by isoflurane inhalation (2% for introducing and 4% for continuous anaesthesia) at 0.6 L/min. MI model was established by left anterior descending coronary artery ligation according to the protocols of our previous study.¹⁴ Diabetic rats were subjected to MI modelling 16 weeks after STZ injection.

Primary myocytes isolation and treatment

The primary myocytes were isolated from neonate male SD rats in accordance with the protocol described by our

FIGURE 1 (A) Left: the heat map of abnormally altered expression of several genes identified in diabetic heart by microarray analysis. Right: the normalized intensities of SLN in microarray analysis. (B) Columns indicate the rat HbA1c% levels 0, 10, and 16 weeks after STZ injections. (C) Columns indicate the relative expression levels of SLN mRNA in rat myocardium 0, 10, and 16 weeks after STZ injections. (D) Left: the immunoblots of SLN and β -actin in rat myocardium 0, 10, and 16 weeks after STZ injections. Right: the relative protein expression levels of SLN in rat myocardium 0, 10, and 16 weeks after STZ injections. (E) Fluorescence immunohistochemistry staining and fluorescent intensities of SLN in myocardium harvested from rats at 0, 10, and 16 weeks after STZ injections. [$n = 6$; * difference were statistically significant ($P < 0.05$)].



previous study.¹⁵ After the myocytes were plated over monolayer confluence at 70%, cells were exposed to whether normal glucose concentration (5.5 mmol/L) or high-glucose concentration (33 mmol/L) for 48 h in accordance to our previous study.¹⁵

Haemodynamic evaluations

The cardiac functions were evaluated by an invasive method in accordance to the protocol described in our previous investigation.¹⁶ Animals were anaesthetized by isoflurane

inhalation and fixed in a supine position. The right carotid artery was exposed and intubated with a Mikro Tip catheter transducer (Millar Instruments) that was inserted into LV. The transducer was connected to Powerlab 4/25 Biological Analysis System (AD Instrument). Systolic haemodynamic parameters including LV systolic pressure (LVSP), maximum (+LVdp/dt), and minimum (−LVdp/dt) derivatives of LV pressure were measured.

Gene expression microarray

By using the RNAeasy™ Plus Animal RNA Isolation Kit (Beyotime), RNAs were extracted from ventricle tissues harvested from rats received intraperitoneal injections of physiological saline as control, 10-week diabetes (10 weeks after STZ injection), and 16-week diabetes (16 weeks after STZ injection), respectively. Integrity and concentration of RNA were assessed prior to labelling. Total RNA from each sample was amplified and transcribed into fluorescent cRNA by using the manufacturer's Agilent's Quick Amp Labeling protocol (version 5.7, Agilent Technologies). The labelled cRNAs were hybridized onto the Whole Genome Oligo Array (4x44K, Agilent Technologies). After having washed the slides, the arrays were scanned by the Agilent Scanner G2505C. Agilent Feature Extraction software (version 11.0.1.1) was used to analyse acquired array images. Quantile normalization and subsequent data processing were performed using the GeneSpring GX v12.0 software package (Agilent Technologies). Differentially expressed genes were identified through Fold Change filtering.

pAAV-tdTomato-SLN siRNA construction, packaging, identification, purification, and delivery

pAAV-tdTomato-SLN siRNA plasmid construction

The rat SLN mRNA sequence was obtained from GenBank. Sequences of three candidate SLN-specific siRNAs (named SLN-111, SLN-170 and SLN-235, respectively) were designed by siRNA software (Ambion) and synthesized by GenePharma. Sequence for SLN-111 was 5'-CCCAGGAGCUGUUUAUCAATTUUGAUAAACAGCUCCUGGGT-3'; for sln-170 was 5'-CUCGUAGGUACCAUTTAUUGGUAGGACCUCACGAGT-3'; and for sln-235 was 5'-GAGCUUCCACUGCUCUGUUTTAACAGAGCAGUGGAAGCUCTT-3'. Sequence for scramble siRNA was 5'-UUCUCCGAACGUGUCACGUTT-3'. The homology of sequence was confirmed by the online homologous sequence index in the National Center for Biotechnology Information. BamHI and HindIII enzymes (NEB) were used to digest and linearize pAAV-tdTomato-shRNA (TaKaRa), which was then ligated to SLN-siRNAs. Products were then transformed into competent cells JM109 and further cultured in LB medium containing

Ampicillin. The recombinant plasmids were extracted by Plasmid Preparation Kit (Beyotime) and identified by BglII enzyme (NEB) digestion and DNA sequencing.

AAV9-tdTomato-SLN siRNA packaging and purification

AAV293 cells were cultured in high-glucose DMEM medium (Gibco) supplemented with 10% foetal bovine serum (Gibco) at 37°C with 5%CO₂/95% fresh air in a humidified incubator. When reached confluence above 60%, the pAAV-tdTomato-SLN siRNA plasmids were transfected into the cells by using calcium phosphate method. An inverted fluorescent microscope was used to observe the fluorescence of Tomato to confirm the successful transfections. The viral supernatant was collected 72 h after packaging by centrifugation and further purified ViraBind™ AAV Purification Mega Kit (Cell Biolabs) per manufacturer's instructions. Viral titre was determined by quantitative polymerase chain reaction (qPCR) in accordance with previous descriptions.

Virus delivery

A 100-μL (2×10^{11} GC/mL) virus preparation was delivered to animals by tail vein injection prior to the establishment of diabetes or MI models. Moreover, tail vein injections of saline were considered as control. Virus were delivered to isolated myocytes at 2×10^7 GC/mL by incubating with myocytes in DMEM medium supplemented with 10% foetal bovine serum at 37°C with 5%CO₂/95% fresh air for 48 h prior to high-glucose exposure.

In vivo distribution and toxicity assessments of AAV9-tdTomato SLN-siRNA

The distribution of AAV9-tdTomato SLN-siRNA in vital organs including heart, lung, liver, kidney, skeletal muscle, and spleen was evaluated 6 weeks after injection of virus preparation. Hearts, lung, liver, kidney skeletal muscle, and spleen were harvested after rats were sacrificed by CO₂ asphyxiation. Tissues were minced and embedded with optimal cutting temperature compound (Sakura) on dry ice. The tissues were sliced and made into 5-μm thick cryostat slides. An inverted fluorescence microscope was used to observe the expression of Tomato, which indicated the distribution of viral vectors. Serum was separated from harvested blood samples. Electrolytes levels including Na⁺, K⁺, and Cl⁻, levels of biochemical markers including creatinine (Cr), blood urea nitrogen, aspartate aminotransferase, alanine aminotransferase, brain natriuretic peptide troponin I (cTnl), and creatine kinase MB isoenzyme were detected at 1, 3, and 6 weeks after injections of virus preparations.

Immunohistochemistry and immunofluorescence staining

Immunohistochemistry and immunofluorescence staining were carried out as described previously.¹⁴ Rat heart ventricle tissue and human cardiac tissue were fixed with 4% (w/v) paraformaldehyde. Tissues were then dehydrated, embedded, and made into 5- μ m sections. After blocking, the sections were incubated with primary antibodies against SLN (1:1000, Abcam) and SERCA2a (1:1000, Abcam), respectively, at 4°C for 8 h. Then the sections were further incubated with secondary antibodies labelled by horseradish peroxidase (Abcam), Alexa Fluor488 (Molecular Probes), and Alexa Fluor594 (Molecular Probes), respectively. Nuclei were tagged with DAPI. The images were visualized and captured by using an inverted microscope.

Real-time quantitative polymerase chain reaction

Total RNA was extracted from myocytes, and SuperScript™ III reverse transcriptase (Invitrogen) was used to synthesize the cDNA according to the protocol provided by the manufacturer. NanoDrop spectrophotometer (Thermo) was used to evaluate the purity and concentration of cDNA. PCR was performed by using HotStarTaq Master Mix Plus (Qiagen) by following the instructions provided by the manufacturer. Primers were synthesized by TaKaRa. Primer sequence for SLN was forward: 5'-GACGTGAAGACGAGCCAGTG-3'; reverse: 5'-CAGCATCCCATGTCAACAGA-3'. Primer sequence for SERCA2a was forward: 5'-TTTTCCGTTACCTGGCTAT-3'; reverse: 5'-CAGCATCCCATGTCAACAGA-3'. Primer sequence for β -actin SLN was forward: 5'-CACGATGGAGGGCCGACTCATC-3'; reverse: 5'-TAAAGACTCTATGCCAACACAGT-3'. After denaturing at 95°C for 5 min, each reaction was carried out with a touchdown PCR protocol for 15 cycles. The annealing temperatures were ranging from 50°C to 65°C, and the extension temperature was 72°C. The quantitative PCR was carried out by using SYBR green/Fluorescein qPCR Master Mix (Thermo). Relative expression levels were analysed by the $2^{-\Delta\Delta C_t}$ method with ViiA7 Quantitative PCR System (Applied Biosystems).

DNA extraction, chemical modification, and bisulfite sequencing

A DNA extraction kit (TianGen) was used to extract DNA from prepared myocytes according to the instruction provided by the manufacturer. EZ DNA methylation-gold kit (Zymo) was used to implement the bisulfite chemical modification of DNA samples. Protocols were carried out by following the manufacturer's instructions. Primers sequence of SLN promoter methylation was designed by TaKaRa as: forward 5'-AAATAAGTTGGTAAGAGTTTGGAGG-3' and reverse 5'-CCCA

AAAAACAAAATAAACACAAT-3'. After denaturing at 95°C for 5 min, each reaction was carried out with a touchdown PCR protocol for 10 cycles. The annealing temperatures were ranging from 50°C to 65°C, and the extension temperature was 72°C. Gel electrophoresis separation (Promega) was used to purify the PCR products, which were then linked to PMD19-T vectors (TaKaRa). After amplification and identification, DNA was extracted and sequenced.

Cytoplasmic calcium ([Ca²⁺]_i) evaluation

reshly prepared cardiac cryostat slides were incubated with the calcium indicator 10 μ mol/L Fura-2/AM (Beyotime) at room temperature in a humidified dark chamber for 30 min. After PBS washing for three times, samples were exited at 340 nm, and the fluorescence of Fura-2/AM was observed at 510 nm with an inverted fluorescence microscope. Quantification of [Ca²⁺]_i was presented as mean fluorescent intensity. For isolated myocytes, the cells were incubated with 5 μ mol/L Fura-2/AM (Thermo) at 37°C for 30 min in dark. The fluorescent intensity of Fura-2/AM was detected by a flow cytometer (BD).

Sarcoplasmic reticulum membrane fraction preparation and SERCA2a activity assay

The SR membrane fraction was acquired by subcellular fractionation in accordance with our previous study¹¹ with several modifications. Briefly, myocytes and minced ventricular tissue were homogenized in isolation buffer I (pH = 7.0) containing 30 mmol/L Tris-maleate (Sigma-Aldrich), 0.3 mol/L sucrose (Sigma-Aldrich), 5 mg/L leupeptin (Sigma-Aldrich), and 0.1 mmol/L PMSF (Santa Cruz). Supernatant was collected after centrifugation at 5500 g for 10 min at 4°C. Then the result pellet was collected after the supernatant was centrifugated at 12 000 g for 20 min at 4°C. The pellet was re-homogenized in isolation buffer II (pH = 7.0) containing 30 mmol/L Tris-maleate, 0.3 mol/L sucrose, 5 mg/L leupeptin, 0.1 mmol/L PMSF, and 0.6 mol/L KCl. The pellet was collected after centrifugation at 143 000 g for 45 min at 4°C, which was then re-homogenized in store buffer (pH = 7.0) containing 30 mmol/L Tris-maleate, 0.3 mol/L sucrose, 5 mg/L leupeptin, 0.1 mmol/L PMSF, and 0.1 mol/L KCl and stored in -80°C. The enzymatic activity of SERCA2a was determined by a colorimetric method by using Ca²⁺-ATPase assay kit (Jiancheng) according to manufacturer's instructions.

Myocytes calcium spark, calcium re-uptake, and cell shortening detections

The calcium spark was detected in isolated myocytes by confocal optical calcium imaging according to the methods

described previously.¹⁷ Isolated myocytes were loaded with 10 $\mu\text{mol/L}$ Fluo3/AM for 30 min at 37°C in dark. After washing by PBS for two times, calcium sparks were observed with an SP8 STED confocal microscope (Leica) equipped with an argon laser at wave length at 488 nm. Line scan was used to acquire the line scan images (512 pixels per line) at sampling rate of 2 ms per line. The scanning frequency was 600 Hz. Calcium sparks were analysed by ImageJ with SparkMaster Plugin according to previously described method.¹⁸ Calcium transients were triggered by MyoPacer (IonOptix) at 0.5 Hz and 40 V at 23°C. Calcium re-uptake was assessed by calculating calcium removal time constant (τ) by using IonWizard software (IonOptix). Cell shortening was measured by using an edge detection system (Crescent Electronics). Cell shortening was presented as percentage of contractile cell length/resting cell length.

Western blotting

Isolated myocytes and minced ventricular tissue were homogenized and lysed by RIPA lysis buffer system (Santa Cruz). Protein was extracted by using Total Protein Extraction kit (Beyotime) according to manufacturer's instructions. A BCA kit (Pierce) was used to determine the concentration of protein. Protein was subjected to sodium dodecyl sulfate polyacrylamide gel electrophoresis. The separated protein was electronically transferred to PVDF membranes. Membranes were incubated with QuickBlock™ blocking buffer (Beyotime) to eliminate the non-specific bindings. Specific antibodies against SLN (1:1000, Abcam), SERCA2a (1:1000, Abcam), and β -actin (1:5000, Abcam) were used to incubate the membranes at 4°C for 10 h and then washed by TBST for five and six times. HRP-conjugated secondary antibodies (1:50 000, Abcam) was used to incubate the membranes at 37°C for 2 h and then washed by TBST for five and six times. ECL kit (Pierce) was used to develop the membranes, and the immunoblots were visualized with Gene Genius System (Syngene).

Cohort study

In the period from May 2017 to May 2019, 101 patients diagnosed as STEMI at Shaanxi Provincial People's Hospital and Heyang County People's Hospital were included. STEMI was diagnosed by the current guideline.¹⁹ DM was diagnosed according to current guideline.²⁰ Cardiac functions were assessed by echocardiography. The exclusion criteria were age below 18 years or above 80 years, pregnant women, previous MI history, previous PCI/CABG history, renal failure, hepatic dysfunction, known history of cancer, immune-mediated disorders, and mental disorders. Human cardiac LV tissue samples was obtained from six STEMI patients undergoing CABG surgery, six STEMI patients

complicated with DM undergoing CABG surgery, and six patients without coronary heart disease and DM undergoing mitral valve replacement operations. All of the patients gave informed consent to participate in this study, which was approved by the Ethics Committee of Shaanxi Provincial People's Hospital (Ref. 201701060-R1) and Ethics Committee of Heyang County People's Hospital (E00251). Specifically, patients signed the informed consent and agreed the collection and research purposes of cardiac LV tissue samples for our investigation. Cardiac tissues were then subjected to immunofluorescence staining as described previously.

Statistics

Data acquired in this study were presented in (mean \pm standard deviations) or percentage manner. Number of independent experiments carried out was indicated as *n*. *NSK* tests were performed as post-hoc tests. Participants were divided into two groups (diabetes and non-diabetes). The baseline characteristics among the two groups were analysed by *t*-test for parametric variables, the Mann-Whitney *U* test for nonparametric variables, and the chi-square test for categorical variables. The Spearman rank correlation coefficient was computed to assess correlation between continuous variables. The association between HbA1c and LVEF were estimated with univariate and multivariate logistic regression models. Model 1 was unadjusted. Model 2 was adjusted for age, sex, body mass index, and cigarette smoking. Model 3 was adjusted for age, sex, body mass index, cigarette smoking, creatinine, UA, low density lipoprotein, K^+ , Na^+ , and troponin I. All statistical testing was two sided. Results were considered statistically significant when $P < 0.05$. All analyses were performed with PASW Statistics 20.0 software.

Results

Screening and identification of sarcolipin expression alteration in diabetic hearts

Cardiac tissues were sampled 10 and 16 weeks after introduction of diabetes by STZ, respectively. As demonstrated in *Figure 1A*, the HbA1c% levels increased significantly in a time-dependent manner. RNA was extracted from the rat LV tissue, and the differentially expressed genes were screened by microarray analysis. The expression level of SLN (Genbank: NM_001013247) was found increased in LV along with the increased HbA1c% levels (*Figure 1B*). The SLN mRNA expression and SLN protein expression alterations in diabetic LV tissue were confirmed by qPCR, western blotting, and fluorescence immunohistochemistry, respectively (*Figure 1EC–1*).

Down-regulation of DNMTs reduced SLN promoter DNA methylation in diabetic left ventricle

Compared with sham control and MI rats, expression levels of two DNMTs, namely, DNMT1 and DNMT3a, reduced significantly in LV tissue sampled from diabetic MI rats (Figure 2A). Bisulfite sequencing DNA methylation analysis spotted six methylation sites of SLN promoter (Supporting Information, Table S1). MI diabetic rats showed the highest demethylation rate of SLN promoter at 55.56%, which was significantly higher than sham control (25.00%) and MI (27.78%) rats (Figure 2B).

Effective silencing of sarcolipin expression by AAV9-tdTomato-SLN siRNA *in vitro* and *in vivo*

Three candidate SLN-siRNAs were connected to pAAV-tdTomato-SLN siRNA plasmids and packaged as AAV9-tdTomato-SLN siRNAs (Supporting Information, Figure S1A and S1B). Virus carrying SLN-111 showed the most potent inhibitory effects on SLN expression than other candidates (SLN-170 and SLN-235) both *in vivo* and *in vitro* (Supporting Information, Figure S1C and S1D). Thus, AAV9-tdTomato-SLN siRNA carrying SLN-111 was used for the subsequent experiments. Six weeks after delivery, AAV9-tdTomato-SLN

siRNA was mainly distributed in heart and barely distributed in other vital organ including liver, kidney, lung, spleen, and skeletal muscle (Supporting Information, Figure S1E). AAV9-tdTomato-SLN siRNA showed bare *in vivo* toxicity because no obvious changes of the biochemical markers were found at 1, 3, and 6 weeks after delivery (Supporting Information, Table S2).

Sarcolipin depletion attenuated left ventricular systolic dysfunctions in diabetic myocardial infarction rat model

SLN expression was significantly up-regulated in LV tissue of diabetic animals (Figure 3A–C). The LV systolic functions were presented by invasive haemodynamic LV measurements. LVSP, +LVdp/dt, and –LVdp/dt decreased dramatically in MI compared with sham. Moreover, highest reduction of LVSP, +LVdp/dt, and –LVdp/dt were found in DM + MI (Figure 3D–F). AAV9-tdTomato-SLN siRNA significantly depleted SLN expression in LV of DM + MI (Figure 3A–C). LV SLN silencing significantly attenuated LVSP, +LVdp/dt, and –LVdp/dt reduction in DM + MI. However, SLN silencing failed to show significant attenuating effects on LV dysfunctions on MI rats compared with sham control (Figure 3D–F).

FIGURE 2 (A) The immunoblots of DNMT1, DNMT3a, and β -actin in cardiac tissue harvested from sham control, myocardial infarction (MI) rat models, and diabetic MI rat models (MI + DM), respectively. Columns indicate the relative expression levels of DNMT1 and DNMT3a in rat myocardium. (B) Calculated demethylation rate of SLN promoter DNA in cardiac tissue harvested from sham, MI, and MI + DM, respectively. [$n = 6$; * difference were statistically significant ($P < 0.05$)].

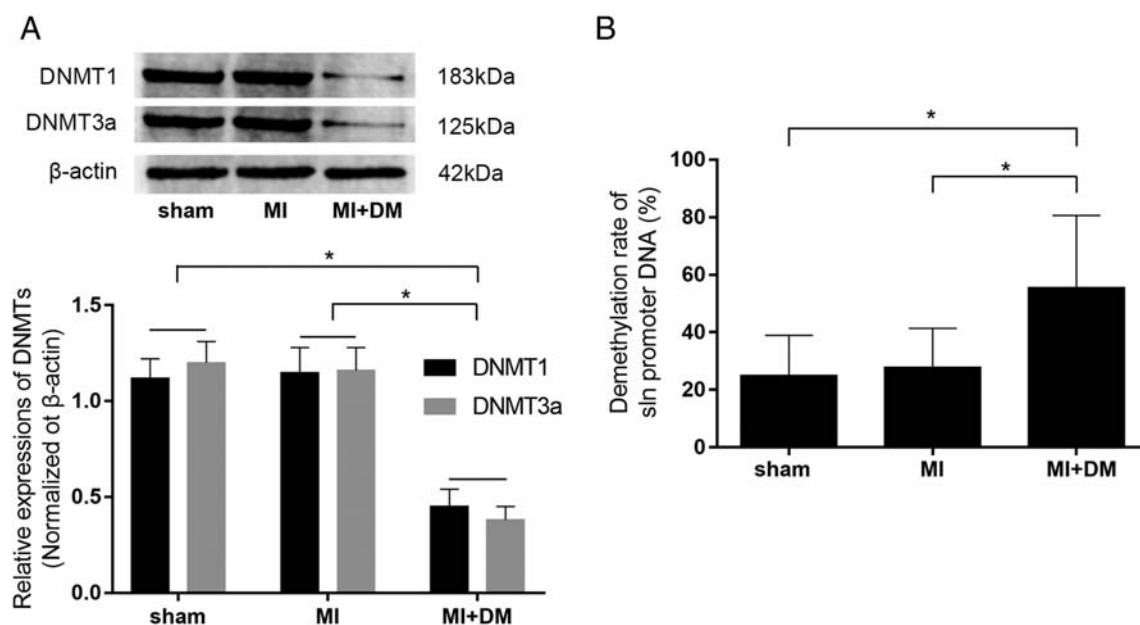
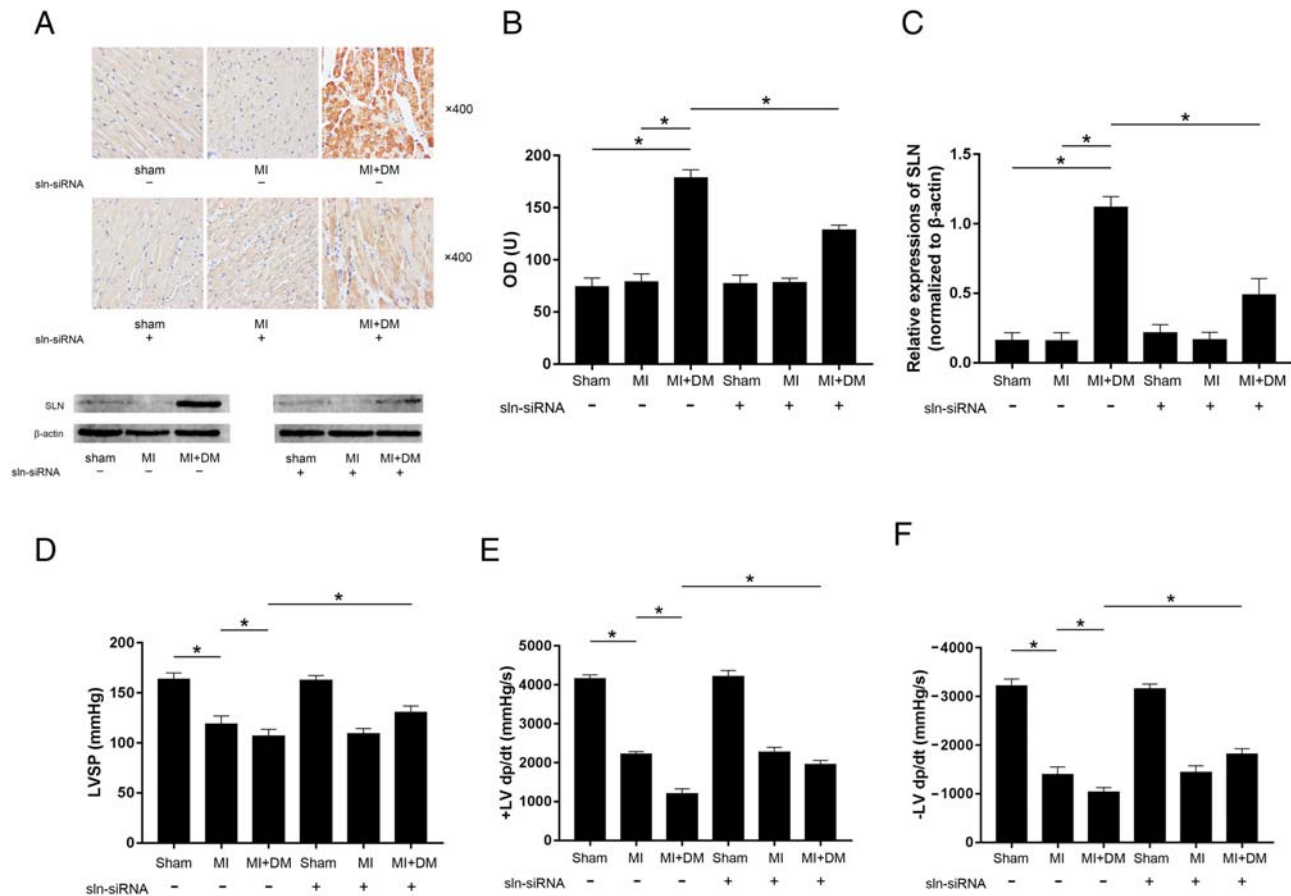


FIGURE 3 (A) The captured images of immunohistochemistry staining of SLN and the immunoblots of SLN and β -actin in cardiac tissue sampled from sham, MI, and MI + DM, respectively. (B) Columns indicate the optical density (OD) of immunohistochemistry staining of SLN. (C) Columns indicate the relative expression levels of SLN (normalized to β -actin). (D–F) Columns indicate the detected haemodynamic parameters (LVSP, +LV dp/dt, and –LV dp/dt) in sham, MI, and MI + DM, respectively. [$n = 10$; * difference were statistically significant ($P < 0.05$)].



Sarcoplipin depletion recovered SERCA2a activity and suppressed $[Ca^{2+}]_i$ elevation in myocardial infarction left ventricles

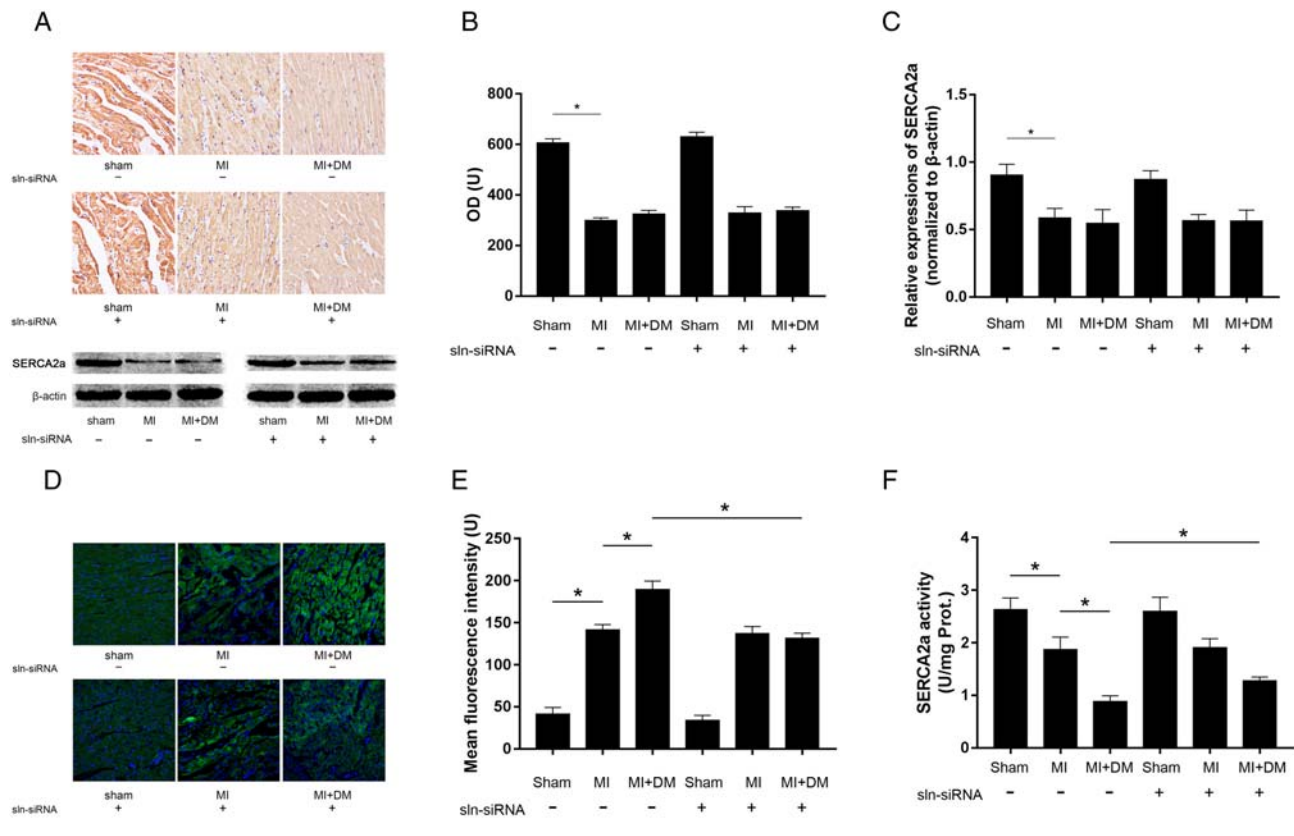
Evidenced by both immunohistochemistry and western blotting, the expression levels of SERCA2a significantly reduced in LV tissue from MI and MI + DM compared with sham, which decreased more significant in LV tissue from MI + DM than MI (Figure 4A). Suggested by the calcium indicator Fura-2/AM, $[Ca^{2+}]_i$ increased significantly in LV tissue from MI and more significantly in MI + DM (Figure 4B). An obvious reduction of SERCA2a activity was observed in LV tissue from MI and more significant in MI + DM (Figure 4C). The knock-down of SLN showed no dramatic effects on the expression levels of SERCA2a in LV tissue from sham, MI, and MI + DM (Figure 4A). However, the knock-down of SLN increased SERCA2a activities in LV tissue from both MI and MI + DM (Figure 4D). Moreover, SLN depletion obviously

reduced $[Ca^{2+}]_i$ in LV tissue from MI + DM without affecting $[Ca^{2+}]_i$ in sham and MI (Figure 4B).

Sarcoplipin depletion increased SERCA2a activity, reduced $[Ca^{2+}]_i$, suppressed calcium sparks, and decreased calcium re-uptake and cell shorting in high-glucose incubated primary myocytes

Isolated primary myocytes were exposed to high-glucose incubation to simulate circumstance of DM. Compared with control, expression levels of SLN increased significantly in myocytes exposed to high-glucose incubation (Supporting Information, Figure S2A). High-glucose incubation decreased the expression levels of SERCA2a in myocytes (Supporting Information, Figure S2B). High-glucose incubation dramatically suppressed SERCA2a enzymatic activity (Supporting Information, Figure S2C), increased $[Ca^{2+}]_i$ (Figure

FIGURE 4 (A) The captured images of immunohistochemistry staining of SERCA2a and the immunoblots of SERCA2a and β -actin in cardiac tissue sampled from sham, MI, and MI + DM, respectively. (B) columns indicate the optical density (OD) of immunohistochemistry staining of SERCA2a. (C) Columns indicate the relative expression levels of SERCA2a (normalized to β -actin). (D) fluorescent images of calcium indicator Fura2/AM staining in fresh cardiac tissue sampled from sham, MI, and MI + DM, respectively. (E) Columns indicate the mean fluorescence intensities of Fura2/AM indicating $[Ca^{2+}]_i$. (F) columns indicate SERCA2a enzymatic activities in each group. [$n = 10$; * difference were statistically significant ($P < 0.05$)].



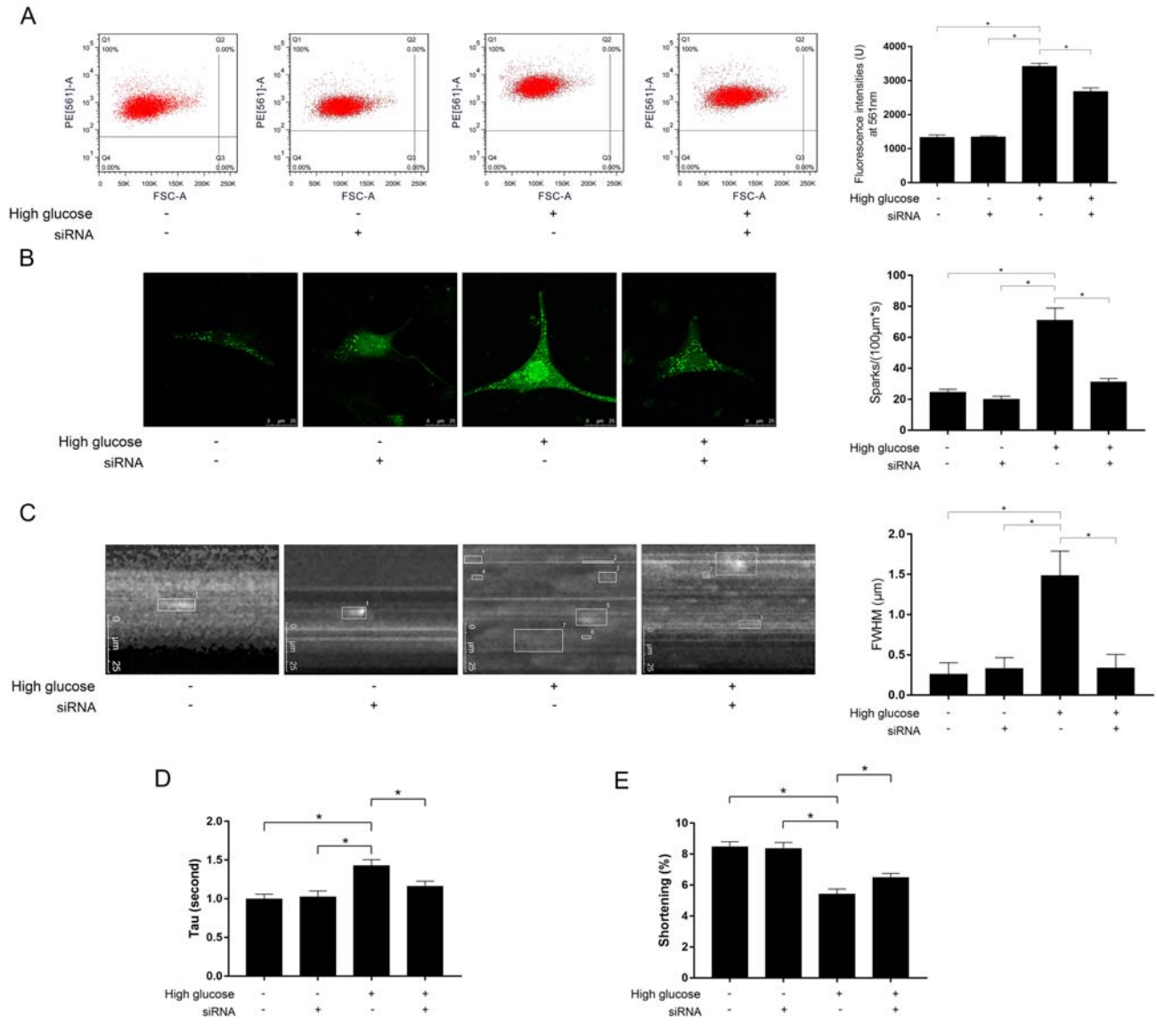
5A), calcium sparks (Figure 5B and 5C), impaired SR calcium re-uptake, and myocyte contractility in high-glucose exposed myocytes. AAV9-tdTomato-SLN siRNA transfection significantly depleted SLN expression in myocytes (Supporting Information, Figure S2A). The SLN depletion significantly increased SERCA2a enzymatic activity (Supporting Information,) without affecting SERCA2a expression levels. SLN silencing decreased $[Ca^{2+}]_i$ (Figure 5A), calcium sparks (Figure 5B and 5C), improved SR calcium re-uptake ability (Figure 5D), and contractility (Figure 5E) in high-glucose exposed myocytes.

Sarcolipin was highly expressed in human cardiac tissue from diabetic ST-segment elevated myocardial infarction patients who exhibited impaired cardiac systolic functions

SLN expression levels in cardiac tissue sampled from patients without coronary heart disease and diabetes, STEMI patients without diabetes, and STEMI patients complicated with

diabetes were analysed. Expression level SLN was significantly up-regulated in diabetic heart compared with non-diabetic hearts (Figure 6A). Population data were successfully obtained from 101 STEMI patients. The baseline data were listed in Table 1. STEMI patients were divided into diabetes group and non-diabetes group. The LVEF% was significantly lower in diabetes group than non-diabetes group (Figure 6B). Spearman rank correlation was used to analyse the association between LVEF% and HbA1c% level, which reflects hyperglycaemia in the past 1–3 months. LVEF% and HbA1c% were significantly related ($r = -0.218$, $P = 0.028$) (Figure 6C). The univariate and multivariate logistic regression models were used to further evaluate the association between LVEF% and HbA1c% in STEMI patients. As demonstrated in Supporting Information, Table S3, in univariable Cox regression model (Model 1), HbA1c% was negatively correlated with LVEF% (OR = 0.77, 95% CI 0.66–0.91, $P < 0.001$). Results of multivariate analysis suggested HbA1c% was negatively and independently correlated with LVEF% (adjusted OR = 0.75, 95% CI 0.63–0.89, $P = 0.001$) after adjusting for age, sex, body mass index, and cigarette smoking (Model 2).

FIGURE 5 (A) Charts of flow cytometry and fluorescent intensities of calcium indicator Fura-2/AM indicating the $[Ca^{2+}]_i$ in high-glucose incubated myocytes treated with AAV9-tdTomato-SLN siRNA. (B) Captured images of calcium sparks and comparisons of spark incidence in high-glucose incubated myocytes treated with AAV9-tdTomato-SLN siRNA. (C) Captured images of assessing spark amplitude and comparisons of full width at half-maximum (FWHM) in high-glucose incubated myocytes treated with AAV9-tdTomato-SLN siRNA. (D) Columns indicate calcium removal time constant (Tau) in each group; (E) Columns indicate myocytes shortening in each group, respectively [$n = 10$; * difference were statistically significant ($P < 0.05$)].



The results were similar in Model 3 (adjusted OR = 0.75, 95% CI 0.62–0.90, $P = 0.002$) after adjusting for age, sex, body mass index, cigarette smoking, creatinine, UA, low density lipoprotein, K+, Na+, and troponin I.

Discussion

According to previous studies, the incidence of HF in hospitalized AMI patients varies from 14–36%.²¹ The degree of HF is

strongly associated with the mortality of AMI patients.²² It has been well established that diabetes is a significant risk factor for major adverse cardiovascular event such as stroke and MI. DM patients complicated with AMI exhibited worse outcomes compared with non-diabetic patients.²³ Previous investigation pointed out that sustained hyperglycaemia during hospitalization was an independent predictor of all-cause mortality in high-risk cardiac patients.²⁴ One of our previous studies has also established the association between impaired cardiac functions and uncontrolled sustained

FIGURE 6 (A) Captured images of SLN fluorescence immunohistochemistry staining of human cardiac tissue sampled from patients diagnosed as degenerative valvular disease (without diabetes and coronary arterial disease, $n = 6$), patients diagnosed as ST-segment elevation myocardial infarction (STEMI) without diabetes ($n = 6$), and patients diagnosed as STEMI complicated with diabetes ($n = 6$) who were undergoing cardiac surgeries. (B) Comparisons of left ventricular ejection fraction (LVEF%) in diabetic and non-diabetic STEMI patients. (C) The correlation analysis between HbA1c% and LVEF% in STEMI patients.

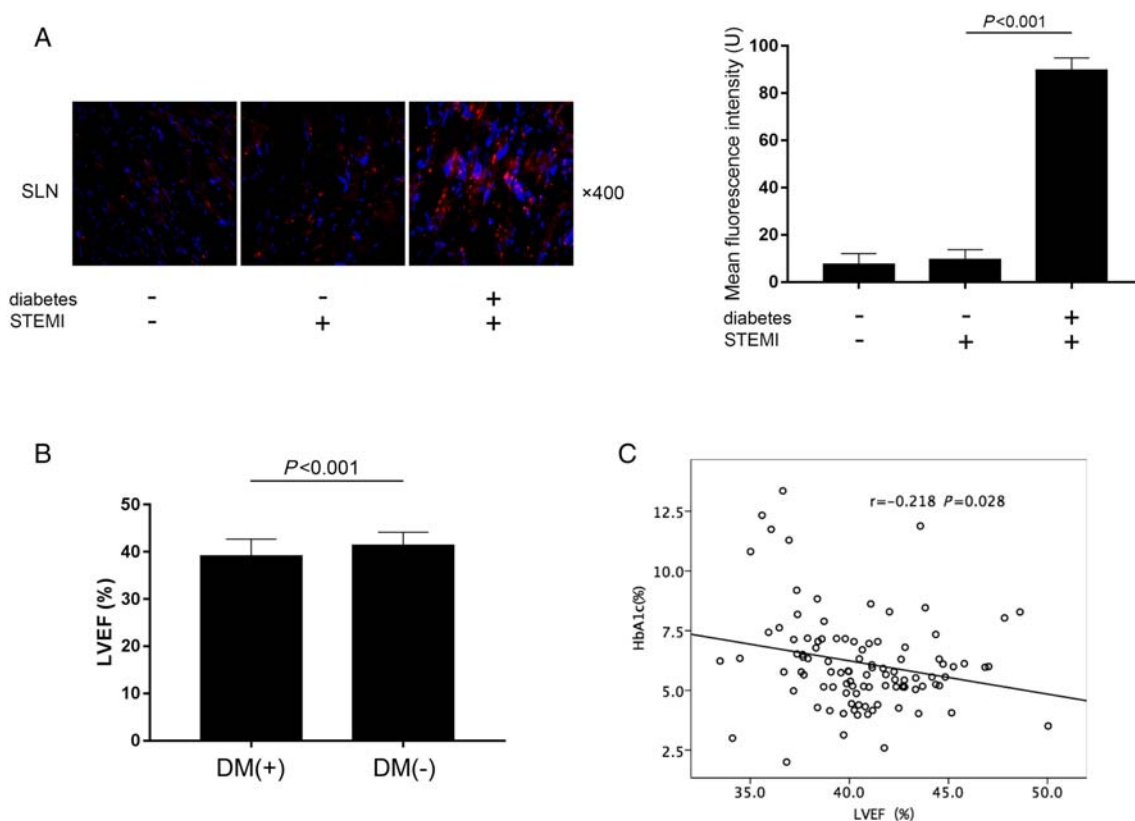


Table 1 Baseline clinical characteristics of the study patients

	Total (n = 101)	DM(-) (n = 67)	DM(+) (n = 34)	P value
Age (year)	53.54 \pm 4.64	54.21 \pm 4.36	52.21 \pm 4.93	0.052
Male (%)	62(61.4)	42(62.7)	20(58.8)	0.829
BMI (kg/m ²)	24.12 \pm 1.42	24.12 \pm 1.45	24.10 \pm 1.37	0.963
Smoking history (%)	38 (37.6)	27 (40.3)	11(32.4)	0.517
Mean heart rate/24 h (bpm)	69.56 \pm 9.93	70.21 \pm 9.15	68.29 \pm 11.34	0.314
CRE (μ mol/L)	60.60 \pm 7.30	61.12 \pm 7.06	59.56 \pm 7.77	0.291
UA (μ mol/L)	282.75 \pm 41.31	288.16 \pm 43.18	272.09 \pm 35.58	0.071
ALT (U/L)	26.84 \pm 11.11	27.53 \pm 11.40	25.47 \pm 10.55	0.495
AST (U/L)	81.39 \pm 14.97	80.69 \pm 13.98	82.76 \pm 16.88	0.490
LDL (mmol/L)	1.98 \pm 0.74	2.08 \pm 0.74	1.78 \pm 0.73	0.097
K ⁺ (mmol/L)	4.26 \pm 0.31	4.25 \pm 0.33	4.29 \pm 0.26	0.433
Na ⁺ (mmol/L)	138.10 \pm 2.50	138.01 \pm 2.30	138.26 \pm 2.90	0.977
Troponin I (ng/mL)	5.36 \pm 3.31	5.20 \pm 3.02	5.67 \pm 3.85	0.736
QTc interval (ms)	426.42 \pm 11.26	426.51 \pm 10.47	426.24 \pm 12.84	0.838
HbA1c (%)	6.15 \pm 2.00	5.10 \pm 0.96	8.20 \pm 1.92	<0.001
LVEF (%)	40.64 \pm 3.20	41.40 \pm 2.74	39.15 \pm 3.93	<0.001

ALT, glutamic-pyruvic transaminase; AST, glutamic-oxalacetic transaminase; BMI, body mass index; CRE, creatinine; HbA1c, glycated haemoglobin; LDL, low density lipoprotein; UA, uric acid; PVCs, premature ventricular contractions.

Continuous variables are presented as mean \pm SD; categorical variables are presented as numbers or percentages.

hyperglycaemia in experimental diabetes animal models.⁴ Glycaemic control improved the long-term outcomes and LV mechanical performance of patients with acute coronary syndrome.²⁵ In this study, our population analysis suggested that HbA1c% was significantly associated with LV systolic dysfunctions in STEMI patients. Moreover, worse LV systolic functions were identified in diabetic MI animals compared with non-diabetic MI animals. These results suggested that diabetes might contribute to exacerbating LV dysfunctions in post-MI HF.

We used microarray to screen out the differentially expressed genes by analysing the mRNA expression profiling in diabetic hearts from rats with sustained uncontrolled hyperglycaemia. The abnormal expressions of SLN were screened out. The up-regulation of expression of SLN was associated with hyperglycaemia. Epigenetic changes such as DNA methylation were responsible for molecular dysregulations in diabetes mellitus. The DNA methylation process is performed by DNMTs, which were reported to be abnormally regulated during diabetes.²⁶ In this study, we found that DNMT1 and DNMT3a were down-regulated in diabetic rat hearts. In mammals, methylation takes place at CpG islands that are localized in non-coding regions. Our methylation analysis results indicated that the methylation rate of the promoter of SLN gene was decreased in diabetic hearts, which was caused by the down-regulation of DNMT1 and DNMT3a. As a result, the expression of SLN was up-regulated. Besides, in cardiac tissue from patients with DM, SLN expression was also found dramatically increased.

SERCAs are membrane proteins taking part in transporting calcium from cytoplasm towards SR lumen. By using free energy generated from ATP hydrolysis, this calcium recycling mechanism facilitates calcium store and attenuates intracellular calcium overload. SERCA2a is the predominant isoform of SERCA existing in cardiac muscle. SERCA2a takes responsibility in augmentation of calcium in SR by re-uptaking calcium from cytoplasm, resulting in greater calcium releasing during next depolarization, therefore generating greater myocyte contractility.²⁷ Reduced SERCA2a expressions and activities were found in both MI and diabetic hearts according to previous reports.^{28,29} Indeed, in this study, we found the expressions of SERCA2a were decreased in both MI and diabetic hearts. In addition, greater reduction of SERCA2a expressions and activities were found in diabetic MI hearts.

SERCA2a activity is mainly regulated by two membrane phosphoproteins, namely, SLN and PLN. By populating an ion-free E1 intermediate protonated at residue Glu771 in transport site I of SERCA's transmembrane domain, SLN decreased the calcium affinity and V_{max} of SERCA pump throughout a kinetic cycle.³⁰ SLN was indicated to be involved in regulating intracellular calcium signals. We have also previously shown that the intracellular calcium regulation dysfunction was involved in cardiac dysfunctions in diabetic hearts.³¹ Targeted over-expression of SLN has been proved to reduce

cardiac contractility in mouse heart.¹⁰ In this study, a myocardiotropic viral vector carrying SLN-siRNA was constructed to silence SLN expressions. The results turned out that the SLN silencing significantly improved cardiac systolic functions of post-MI DM animals without affecting non-diabetic post-MI animals. SLN silencing did not change cardiac SERCA2a expressions. Moreover, SLN depletion dramatically recovered SERCA2a activity in diabetic hearts without significantly affecting non-diabetic ones. Thus, we could conclude that SLN participated in impairing cardiac systolic functions through regulating SERCA2a activity in MI complicated with DM exclusively.

It has been established that $[Ca^{2+}]_i$ elevation was highly correlated with heart failure.⁵ Due to reduction of SERCA2a expression, $[Ca^{2+}]_i$ elevated in MI and DM hearts, resulting in impaired cardiac systolic functions. The calcium released through RyRs from SR underlies the $[Ca^{2+}]_i$ elevation in subspace between plasma membrane and SR membrane, which is visualized as calcium sparks. The released calcium further acts as the 'trigger calcium' to a large amount of calcium release and thus underlies a positive feedback called calcium-induced calcium release.³² In our *in vitro* experiments, $[Ca^{2+}]_i$ was dramatically elevated after high-glucose incubation, which further boosted the calcium sparks in a spatio-temporal manner. SERCA2a expression and activity were found significantly suppressed while SLN expression was found dramatically increased in high-glucose incubated myocytes. The SLN depletion recovered SERCA2a activity without affecting SERCA2a expression level in high-glucose incubated myocytes. As a result, SLN depletion attenuated high-glucose induced calcium sparks, improved SR calcium re-uptake ability, and myocytes contractility. These results suggested high-glucose exposure decreased myocyte contractility via impairing SERCA2a-associated SR calcium recycling mechanism. SLN was proved as a key pathogenic factor mediating high-glucose induced cardiac contraction dysfunctions.

Conclusions

DM increases the vulnerability of STEMI patients to HF. Diabetes-associated SLN promoter methylation suppression up-regulated SLN expression, which reduced the SERCA2a activity. As a result, SR calcium re-uptake ability was hindered, leading to $[Ca^{2+}]_i$ elevation and myocytes contractility impairments.

Limitations

There are several limitations of this study. First, in the *in vivo* study, employment of SLN knock-out animals would make the investigation more persuasive. Second, it would be better

if more human cardiac tissue could be sampled. Third, the sample size of our population study was small. Around 101 study subjects were from two medical centres and were limited to the native Chinese population. These aforementioned facts limited the generalizability of our findings.

Perspectives

Post-MI HF often indicates poor cardiovascular outcomes in diabetes patients. Sometimes conventional drugs are also helpless in certain cases. Genetic targeted therapy that is widely applied in oncology would be a promising strategy in treatments of cardiovascular diseases. Previous studies have proposed that increasing SERCA was beneficial in reducing HF. However, very few investigations considering this as a therapeutic strategy were carried out. In this study, we constructed a myocardiotropic viral vector carrying siRNA silencing SLN that was delivered to animals through intravenous injections. The viral vector was mainly delivered to myocardium, which effectively silenced myocardial SLN expression. The administration of the viral vector showed significant improving effects on diabetic post-MI HF. The serum biochemical markers were not obviously altered after viral vector injections. Thus, our data evidenced the targetability, biosafety, and effectiveness of this genetic therapy against post-MI HF in diabetes.

Ethics approval and consent to participate

All animal experimental procedures were carried out according to Recommended Guideline for the Care and Use of Laboratory Animals issued by Chinese Council on Animal Research. The protocols regarding animal experiments were approved by the Medical Animal Research Ethics Committee at Xi'an Jiaotong University (Ref. 201,806,230-R1). All of the patients gave informed consent to participate in this study, which was approved by the Ethics Committee of Shaanxi Provincial Peoples' Hospital (Ref. 201,701,060-R1) and Ethics Committee of Heyang County People's Hospital (E00251). Specifically, patients signed the informed consent and agreed the collection and research purposes of cardiac tissue sample for our investigation.

References

1. Granger CB, Goldberg RJ, Dabbous O, Pieper KS, Eagle KA, Cannon CP, Van De Werf F, Avezum A, Goodman SG, Flather MD, Fox KAA. Global Registry of Acute Coronary Events I. Predictors of hospital mortality in the global

Availability of data and materials

Data are available from the corresponding author on reasonable request.

Conflict of interest

The authors declare that they have no competing interests.

Funding

The study was supported by Fundamental Scientific Research Foundation of Xi'an Jiaotong University (xzy012019131); Innovative Talents Promotion Project of Shaanxi Province (2019KJXX-019); National Natural Scientific Foundation of China (81600646); and Health Research Foundation of Shaanxi Province (2018E011).

Authors' contributions

Z. W. Liu and Y. Zhang implemented experiments and wrote the manuscript; C. Qiu and H. Jia accomplished statistical analysis; S. Pan and G. C. Guan participated in implementing experiments; H. T. Zhu and H. Y. Kang revised the manuscript; L. Zhu designed and participated in the statistical analysis; J. K. Wang and R.T. Hui reviewed and revised the manuscript.

Supporting information

Additional supporting information may be found online in the Supporting Information section at the end of the article.

Figure S1. construction, transfection efficiency and distribution of AAV9-tdTomato-sln siRNA

Figure S2. SLN and SERCA2a expressions and SERCA2a enzymatic activity assessments in primary myocytes transfected with AAV9-tdTomato-sln siRNA

Table S1. Analysis of demethylation site and demethylation rate of SLN promoter in rat cardiac tissue

Table S2. Plasma biochemical markers detection after AAV9-tdTomato-sln delivery in rats

Table S3. Univariate and multivariate logistic analysis as a continuous variable of percentage of HbA1c

- registry of acute coronary events. *Arch Intern Med* 2003; **163**: 2345–2353.
2. Timmer JR, Ottervanger JP, Thomas K, Hoorntje JCA, de Boer M-J, Suryapranata H, Zijlstra F, Zwolle Myocardial Infarction Study G. Long-term, cause-specific mortality after myocardial infarction in diabetes. *Eur Heart J* 2004; **25**: 926–931.
 3. Stone PH, Muller JE, Hartwell T, York BJ, Rutherford JD, Parker CB, Turi ZG, Strauss HW, Willerson JT, Robertson T, The MILIS Study Group. The effect of diabetes mellitus on prognosis and serial left ventricular function after acute myocardial infarction: contribution of both coronary disease and diastolic left ventricular dysfunction to the adverse prognosis. *J Am Coll Cardiol* 1989; **14**: 49–57.
 4. Liu Z-w, Wang J-k, Qiu C, Guan G-c, Liu X-h, Li S-j, Deng Z-r. Matrine pretreatment improves cardiac function in rats with diabetic cardiomyopathy via suppressing ROS/TLR-4 signaling pathway. *Acta Pharmacol Sin* 2015; **36**: 323–333.
 5. Marks AR. Calcium cycling proteins and heart failure: mechanisms and therapeutics. *J Clin Invest* 2013; **123**: 46–52.
 6. Lompré A-M, Hajjar RJ, Harding SE, Kranias EG, Lohse MJ, Marks AR. Ca²⁺ cycling and new therapeutic approaches for heart failure. *Circulation* 2010; **121**: 822–830.
 7. Arai M, Alpert NR, MacLennan DH, Barton P, Periasamy M. Alterations in sarcoplasmic reticulum gene expression in human heart failure. A possible mechanism for alterations in systolic and diastolic properties of the failing myocardium. *Circ Res* 1993; **72**: 463–469.
 8. Autry JM, Thomas DD, Espinoza-Fonseca LM. Sarcolipin promotes uncoupling of the SERCA Ca²⁺ pump by inducing a structural rearrangement in the energy-transduction domain. *Biochemistry* 2016; **55**: 6083–6086.
 9. Asahi M, Kurzydowski K, Tada M, MacLennan DH. Sarcolipin inhibits polymerization of phospholamban to induce superinhibition of sarco (endo) plasmic reticulum Ca²⁺-ATPases (SERCAs). *J Biol Chem* 2002; **277**: 26725–26728.
 10. Babu GJ, Bhupathy P, Petrashevskaya NN, Wang H, Raman S, Wheeler D, Jagatheesan G, Wiecek D, Schwartz A, Janssen PML, Ziolo MT, Periasamy M. Targeted overexpression of sarcolipin in the mouse heart decreases sarcoplasmic reticulum calcium transport and cardiac contractility. *J Biol Chem* 2006; **281**: 3972–3979.
 11. Liu Z, Cai H, Zhu H, Toque H, Zhao N, Qiu C, Guan G, Dang Y, Wang J. Protein kinase RNA-like endoplasmic reticulum kinase (PERK)/calcineurin signaling is a novel pathway regulating intracellular calcium accumulation which might be involved in ventricular arrhythmias in diabetic cardiomyopathy. *Cell Signal* 2014; **26**: 2591–2600.
 12. Dhliwayo N, Sarras MP Jr, Luczkowski E, Mason SM, Intine RV. Parp inhibition prevents ten-eleven translocase enzyme activation and hyperglycemia-induced DNA demethylation. *Diabetes* 2014; **63**: 3069–3076.
 13. Liu ZW, Zhu HT, Chen KL, Dong X, Wei J, Qiu C, Xue JH. Protein kinase RNA-like endoplasmic reticulum kinase (PERK) signaling pathway plays a major role in reactive oxygen species (ROS)-mediated endoplasmic reticulum stress-induced apoptosis in diabetic cardiomyopathy. *Cardiovasc Diabetol* 2013; **12**: 158.
 14. Zhao N, Mi L, Zhang X, Xu M, Yu H, Liu Z, Liu X, Guan G, Gao W, Wang J. Enhanced MiR-711 transcription by PPARγ induces endoplasmic reticulum stress-mediated apoptosis targeting calnexin in rat cardiomyocytes after myocardial infarction. *J Mol Cell Cardiol* 2018; **118**: 36–45.
 15. Liu ZW, Zhu HT, Chen KL, Dong X, Wei J, Qiu C, Xue JH. Protein kinase RNA-like endoplasmic reticulum kinase (PERK) signaling pathway plays a major role in reactive oxygen species (ROS)-mediated endoplasmic reticulum stress-induced apoptosis in diabetic cardiomyopathy. *Cardiovasc Diabetol* 2013; **12**: 1475–2840.
 16. Liu Z, Zhang Y, Tang Z, Xu J, Ma M, Pan S, Qiu C, Guan G, Wang J. Matrine attenuates cardiac fibrosis by affecting ATF6 signaling pathway in diabetic cardiomyopathy. *Eur J Pharmacol* 2017; **804**: 21–30.
 17. Tjondrokoesoemo A, Li N, Lin PH, Pan Z, Ferrante CJ, Shirokova N, Brotto M, Weisleder N, Ma J. Type 1 inositol (1,4,5)-trisphosphate receptor activates ryanodine receptor 1 to mediate calcium spark signaling in adult mammalian skeletal muscle. *J Biol Chem* 2013; **288**: 2103–2109.
 18. Picht E, Zima AV, Blatter LA, Bers DM. SparkMaster: automated calcium spark analysis with ImageJ. *Am J Physiol Cell Physiol* 2007; **293**: C1073–C1081.
 19. Ibanez B, James S, Agewall S, Antunes MJ, Bucciarelli-Ducci C, Bueno H, Caforio ALP, Crea F, Goudevanos JA, Halvorsen S, Hindricks G, Kastrati A, Lenzen MJ, Prescott E, Roffi M, Valgimigli M, Varenhorst C, Vranckx P, Widimsky P. 2017 ESC Guidelines for the management of acute myocardial infarction in patients presenting with ST-segment elevation: the Task Force for the management of acute myocardial infarction in patients presenting with ST-segment elevation of the European Society of Cardiology (ESC). *Eur Heart J* 2018; **39**: 119–177.
 20. 16. Diabetes advocacy: standards of medical care in diabetes-2019. *Diabetes Care* 2019; **42**: S182–s183.
 21. Bahit MC, Kochar A, Granger CB. Post-myocardial infarction heart failure. *JACC Heart Fail* 2018; **6**: 179–186.
 22. Hellermann JP, Jacobsen SJ, Gersh BJ, Rodeheffer RJ, Reeder GS, Roger VL. Heart failure after myocardial infarction: a review. *Am J Med* 2002; **113**: 324–330.
 23. Donahoe SM, Stewart GC, McCabe CH, Mohanavelu S, Murphy SA, Cannon CP, Antman EM. Diabetes and mortality following acute coronary syndromes. *JAMA* 2007; **298**: 765–775.
 24. Lipton JA, Barendse RJ, Van Domburg RT, Schinkel AF, Boersma H, Simoons MI, Akkerhuis KM. Hyperglycemia at admission and during hospital stay are independent risk factors for mortality in high risk cardiac patients admitted to an intensive cardiac care unit. *Eur Heart J Acute Cardiovasc Care* 2013; **2**: 306–313.
 25. Sasso FC, Rinaldi L, Lascar N, Marrone A, Pafundi PC, Adinolfi LE, Marfella R. Role of Tight glycemic control during acute coronary syndrome on CV outcome in type 2 diabetes. *J Diabetes Res* 2018; **2018**: 3106056–3106056.
 26. Sankritiyayan H, Kulkarni YA, Gaikwad AB. Diabetic nephropathy: the regulatory interplay between epigenetics and microRNAs. *Pharmacol Res* 2019; **141**: 574–585.
 27. Abi-Samra F, Gutterman D. Cardiac contractility modulation: a novel approach for the treatment of heart failure. *Heart Fail Rev* 2016; **21**: 645–660.
 28. Talukder MAH, Yang F, Nishijima Y, Chen C-A, Kalyanasundaram A, Periasamy M, Zweier JL. Reduced SERCA2a converts sub-lethal myocardial injury to infarction and affects postischemic functional recovery. *J Mol Cell Cardiol* 2009; **46**: 285–287.
 29. Singh RM, Waqar T, Howarth FC, Adeghata E, Bidasee K, Singh J. Hyperglycemia-induced cardiac contractile dysfunction in the diabetic heart. *Heart Fail Rev* 2018; **23**: 37–54.
 30. Espinoza-Fonseca LM, Autry JM, Thomas DD. Sarcolipin and phospholamban inhibit the calcium pump by populating a similar metal ion-free intermediate state. *Biochem Biophys Res Commun* 2015 Jul 17–24; **463**: 37–41.
 31. Wang J, Tang Z, Zhang Y, Qiu C, Zhu L, Zhao N, Liu Z. Matrine alleviates AGES-induced cardiac dysfunctions by attenuating calcium overload via reducing ryanodine receptor 2 activity. *Eur J Pharmacol* 2019; **842**: 118–124.
 32. Sobie EA, Dilly KW, dos Santos Cruz J, Lederer WJ, Jafri MS. Termination of cardiac Ca²⁺ sparks: an investigative mathematical model of calcium-induced calcium release. *Biophys J* 2002; **83**: 59–78.